2026 IEEE/SICE International Symposium on System Integration (SII)
January 11-14, 2026. Cancún, México

MRF-Based Mapping of Fetal and Maternal Deformations for Understanding and Supporting Fetal Movement Perception

Haruka Matoba[1,†], Takashi Kusaka[2], Koji Shimatani[3],
Dongmin Kim[4], Hoshinori Kanazawa[4], Yasuo Kuniyoshi[4] and Takayuki Tanaka[2]

***Abstract*— This study proposes a foundational method for objectively classifying whether mothers can easily perceive fetal movements, a crucial indicator in perinatal care. Traditional fetal movement assessments rely on subjective maternal reports or wearable sensor-based methods susceptible to external noise. This paper applies the previously established Multi-Resolution Feature (MRF) method to independently quantify both fetal and maternal deformation from simulated fetal movement videos. We constructed a novel fetal-maternal deformation map using these deformation values as axes. The results demonstrate that this map can visually represent the relationship between fetal and maternal deformation. Furthermore, exploratory analysis of the data distribution on the map suggested the existence of distinct fetal movement patterns: movements accompanied by significant maternal abdominal wall deformation (likely perceived by the mother) and movements where the fetus is active but less transmission occurs to the mother (likely difficult for the mother to perceive). This method is expected to be a stepping stone towards establishing a new approach for more detailed assessment of fetal health and, consequently, improving the quality of perinatal medical care.**

I. INTRODUCTION

Fetal movement measurement is crucial for understanding fetal health and promoting mother-child bonding [1], [2]. However, current methods face several challenges. The most common, fetal kick counting, relies on subjective maternal perception [3]. A lack of standardized guidelines further compromises objectivity [4]. Factors like maternal body shape and fetal position also impede objective assessment [5], [6], [7]. Primiparous women, in particular, often misinterpret fetal movements as maternal digestive activity [8]. These subjective assessment limitations significantly hinder accurate fetal health understanding and maternal anxiety alleviation.

*This work was not supported by any organization.

[1] Haruka Matoba is with the Graduate School of Information Science and Technology, Hokkaido University, Sapporo, Japan matoba@hce.ist.hokudai.ac.jp

[2] Takashi Kusaka and Takayuki Tanaka are with the Faculty of Information Science and Technology, Hokkaido University, Sapporo, Japan kusaka@hce.ist.hokudai.ac.jp, ttanaka@hce.ist.hokudai.ac.jp

[3] Koji Shimatani is with the Faculty of Health and Welfare, Prefectural University of Hiroshima, Mihara, Japan shimatani@pu-hiroshima.ac.jp

[4] Dongmin Kim, Hoshinori Kanazawa and Yasuo Kuniyoshi are with Graduate School of Information Science and Technology, The University of Tokyo, Tokyo, Japan d-kim@isi.imi.i.u-tokyo.ac.jp, kanazawa@isi.imi.i.u-tokyo.ac.jp, kuniyosh@isi.imi.i.u-tokyo.ac.jp

† Corresponding author

While accelerometer sensors have been proposed for fetal movement measurement [9], they are susceptible to noise from breathing and maternal movements. To counter this, we propose using ultrasound videos for robust sensing against external disturbances. However, most existing ultrasound video studies focus on detecting movement presence or intensity, struggling to differentiate between perceivable and hard-to-perceive movements. Furthermore, many require expert evaluation, meaning an objective and quantitative fetal movement assessment method remains unestablished [10].

Given this, our study focuses on the physiological aspects of maternal fetal movement perception. The maternal abdomen contains mechanoreceptors that generate sensory input from external pressure changes and local stretching [11]. This makes abdominal wall deformation accompanying fetal movements a primary factor in maternal perception [12]. Thus, quantitatively evaluating maternal abdominal deformation (hereafter "maternal deformation") is useful for detecting fetal movements and understanding perception tendencies. It is hypothesized that fetal movements accompanied by maternal abdominal deformation are more easily perceived by the mother.

This study aims to enable objective classification of fetal movements based on maternal perceptual characteristics, specifically to build a support system presenting perceivable movements to mothers struggling to feel them. The Multi-Resolution Feature (MRF) method is applied to simultaneously calculate fetal and maternal deformation from simulation videos[13]. Subsequently, a novel fetal-maternal deformation map is proposed using these values as axes. The paper's purpose is to visualize the relationship between fetal movement and maternal response with this map, verifying its potential for classifying fetal movement patterns. Specifically, we extracted fetal and maternal deformation from simulated videos to validate the proposed method, laying groundwork for future analysis with real ultrasound data.

II. METHOD

This section proposes a method for constructing a fetal-maternal deformation map to visualize the interaction between fetal activity and maternal perception. We will first present the concept of the proposed fetal-maternal deformation map, then detail the underlying deformation calculation technique, appropriate scale selection, and the construction of the map itself.

978-1-6654-5784-2/26/$31.00 ©2026 IEEE

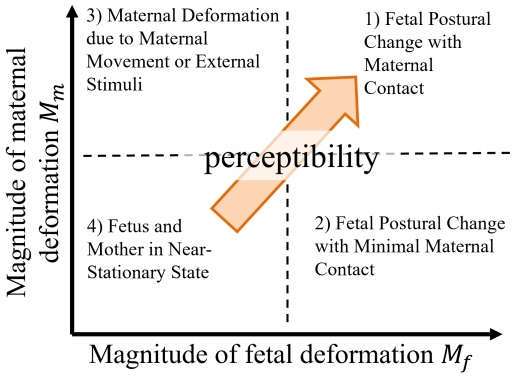

Fig. 1: Overview of fetal and maternal deformation map. M_f and M_m represent the fetal and maternal deformation, respectively, and are defined as a single element or an integration of multiple elements of $\mathbf{M}(\mathbf{S}, t)$.

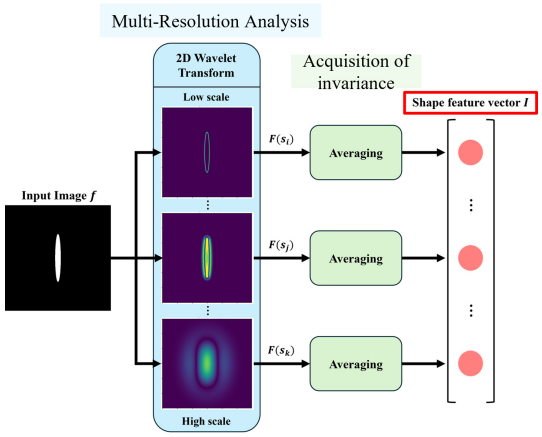

Fig. 2: The overall flow of MRF method, where $s_0 < s_1 < s_2$, which performs frequency analysis and averaging on the input image.

A. Concept of the Fetal-Maternal Deformation Map

The fetal-maternal deformation map proposed in this study is a two-dimensional space defined to integrate fetal and maternal deformation data and objectively evaluate the perceptual characteristics of fetal movement. The method for calculating deformation applies the MRF method proposed in previous research, and the calculation formula will be described later. An overview of the fetal-maternal deformation map is shown in Fig.1. The X-axis of this map represents fetal deformation, and the Y-axis represents maternal deformation. Each data point plotted on the map indicates the relative simultaneous deformation state of the fetus and the mother at a specific moment.

Fetal movements are proposed to be classified into four categories based on the position of data points on this map. This classification aims to distinguish how effectively fetal movements are transmitted to the mother, and whether the movements originate from the fetus itself or from the mother.

1) Prominent maternal deformation caused by fetal movement: A region where both the fetal and maternal axes show large values (clearly perceivable fetal movement). The fetal movement is strong and effectively transmitted to the maternal abdominal wall, making it highly perceivable by the mother.
2) Fetal movement with minimal maternal contact: A region where only the fetal axis shows large values, while the maternal axis remains small (barely perceivable fetal movement). The fetus is actively moving, but has limited contact with the maternal abdominal wall, making the movement difficult for the mother to perceive.
3) Maternal deformation not caused by fetal movement: A region where only the maternal axis shows large values, while the fetal axis remains small (maternal-origin deformation). The deformation is due to maternal movements (such as breathing) or external stimuli and is not triggered by fetal activity.
4) Near-stationary state of both fetus and mother: A region where both fetal and maternal axes show small or near-zero values. This indicates that both the fetus and maternal abdominal wall are nearly stationary, with no significant movement or external interference.

This four-category classification system is believed to be capable of distinguishing fetal-derived movements from maternal-derived movements or external influences, particularly in identifying fetal movements that are difficult to perceive. By representing fetal and maternal deformation on separate axes, it is possible to identify movements originating from the fetus but with limited transmission to the mother, as well as maternal movements that are often mistaken for fetal movements. However, the relationship between maternal deformation and the perception threshold has not yet been clarified, making it difficult to determine the boundaries of these categories.

B. Deformation Calculation using the MRF Method

To construct the fetal-maternal deformation map proposed above, it is first necessary to calculate the objective deformation magnitudes of both the fetus and the mother. The foundational technology for this is the MRF method, which has been established in previous research. A conceptual diagram of the MRF method is shown in Fig.2.

The MRF method extracts shape features at multiple scales for uncertain shapes, independent of position and rotation. The translation- and rotation-invariant shape feature vector $I(s,t)$ at each scale is given by Equation 1.

$$I(s,t) = \frac{1}{W \cdot H} \sum_{h=1}^{H} \sum_{w=1}^{W} |F(s,t,w,h)| \qquad (1)$$

Here, t represents the frame number of the input image, s is the scale parameter, (w,h) denote the pixel displacements in the x and y directions, respectively, W and H represent the width and height of the input image, and $F(s,t,w,h)$

indicates the coefficients obtained by wavelet transform. The mother wavelet is assumed to be isotropic.

The deformation magnitude vector $\mathbf{M}(\mathbf{S}, t)$ is defined by the temporal change of this shape feature vector. Since the features obtained by the MRF method are translation-invariant and rotation-invariant, the calculated deformation magnitude vector $\mathbf{M}$ is not due to the rigid body motion of the deformed object. The deformation magnitude is calculated as the absolute difference of the vectors between consecutive frames, as shown in Equation 2.

$$\mathbf{M}(\mathbf{S}, t) = \{M_1, ..., M_n\} = \{|\Delta I(s_1, t)|, ..., |\Delta I(s_n, t)|\} \tag{2}$$

This deformation magnitude vector $\mathbf{M}$ is defined as a set of vectors whose elements represent the magnitude of deformation at each scale. Each element $M_n = |\Delta I(s_n, t)|$ of the deformation magnitude vector represents the magnitude of deformation at a specific scale s_n . Here, $\mathbf{S}$ is the set of scales, and n indicates the total number of scales in the set. The multi-resolution approach in the MRF method enables capturing deformations at different anatomical scales, from subtle fetal deformations (e.g., arm flexion) to large whole-body deformations (e.g., whole-body extension). This allows for a more comprehensive understanding of the separation of maternal and fetal activity and detailed fetal movements, compared to conventional evaluation methods that can only capture a single scale.

C. Extraction Method for Shape Description Features

When calculating deformation magnitudes using the MRF method, the selection of the analysis scale, i.e., the size of the shape to be analyzed, is crucial. This study adopts a method that automatically identifies scales from the local maxima of the wavelet variance $\sigma^2(s)$. This method has the advantage of automatically identifying the most appropriate scale for shape identification, which most sensitively and effectively reflects changes when a shape transforms.

The shape description features $\mathbf{S}_p$ is expressed as:

$$\mu(s) = \frac{1}{T} \sum_{t=0}^{T} I(s, t) \tag{3}$$

$$\sigma^2(s) = \frac{1}{T} \sum_{t=0}^{T} (I(s, t) - \mu(s))^2 \tag{4}$$

$$\mathbf{S}_p = \left\{ s \mid \frac{d}{ds}(\sigma^2(s)) = 0,\ \frac{d^2}{ds^2}(\sigma^2(s)) < 0 \right\} \tag{5}$$

In these equations, s represents the scale parameter, t is the image number, and T denotes the total number of images.

III. EXPERIMENT

This experiment verifies whether the proposed method can appropriately detect fetal movements as deformation magnitudes in simulated videos, and whether the constructed fetal-maternal deformation map can elucidate the interaction between fetal activity and maternal perception based on these deformation magnitudes. For this purpose, It was confirmed the time-series changes of fetal and maternal deformation and created the fetal-maternal deformation map.

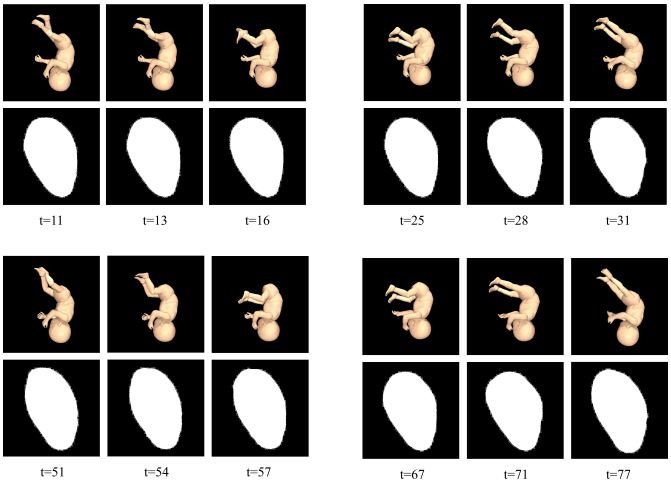

Fig. 3: Simulation images of frames within the fetal and maternal movement onset interval. Images of the fetus at the top and the maternal are displayed at the bottom, arranged vertically. The variable t represents the frame number in the simulation movie.

A. Experimental method

The input data consists of simulated fetal videos generated from a physics-based simulation, in which a musculoskeletal model produced spontaneous movements driven by chaotic oscillators [14]. The videos were consistently rendered from the sagittal plane and include various fetal postures such as flexion and extension (Fig. 3), along with corresponding maternal abdominal surface movements responding to the fetal dynamics. The numbers written at the bottom of each image indicate the frame number. These two videos are input separately to calculate their respective deformation magnitudes. The frame rate is 20 fps, the total number of frames is 90, and the resolution is 500 px per side. Among the fetal movements in the video, movements involving flexion postures occur around frames 11-16 and 51-60, while movements involving extension postures occur around frames 25-31 and 67-75. These fetal movement occurrence times were visually labeled as the period from when the fetus starts moving from a static state until it becomes static again. All maternal deformation in this video is attributed to fetal movement.

IV. RESULTS

A. Extraction of Shape Description Features and Scale Selection

To capture the dynamic behavior of the fetus and mother, scales serving as shape description features were extracted using wavelet variance. The graph of wavelet variance, which expresses the intensity of shape variation at each scale, is shown in Fig. 4.

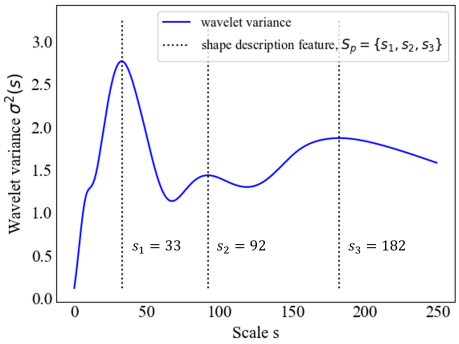

(a) Wavelet variance of the shape feature vectors for all frames by scale by fetal movie.

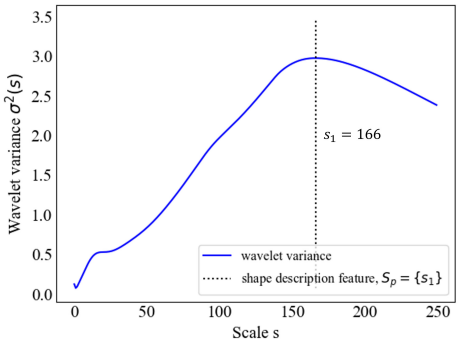

(b) Wavelet variance of the shape feature vectors for all frames by scale by maternal movie.

Fig. 4: Wavelet variance of the shape feature vectors for all frames

Each dotted line in the figures indicates the scale corresponding to a local maximum. From the fetal video, three scales, $\mathbf{S}_p = \{33, 92, 182\}$, were extracted as shape description features. On the other hand, from the maternal video, a single scale, $\mathbf{S}_p = \{166\}$, was extracted as a shape description feature. These extracted scales form the basis for the deformation magnitude calculation described later.

B. Calculation of Fetal and Maternal Deformation

To construct the fetal-maternal deformation map proposed above, it is first necessary to calculate the objective deformation magnitudes of both the fetus and the mother. The foundational technology for this is the MRF method, which has been established in previous research.

The deformation magnitudes for the three scales identified as fetal-derived shape description features contained multi-dimensional and redundant information. Therefore, dimensionality reduction was performed to facilitate analysis and subsequent processing. Specifically, Principal Component Analysis (PCA) was applied to construct the fetal axis, which represents fetal deformation. As a result of this PCA, the contribution ratio of the first principal component was 0.91. On the other hand, the deformation magnitude selected as maternal-derived was limited to a single scale and was adopted directly as the maternal axis.

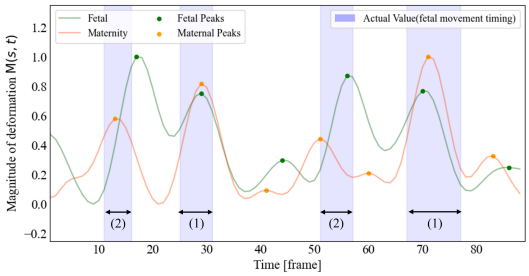

Fig. 5: Time series changes in fetal and maternal deformation. Fetal movement occurrence time is indicated by a blue band.

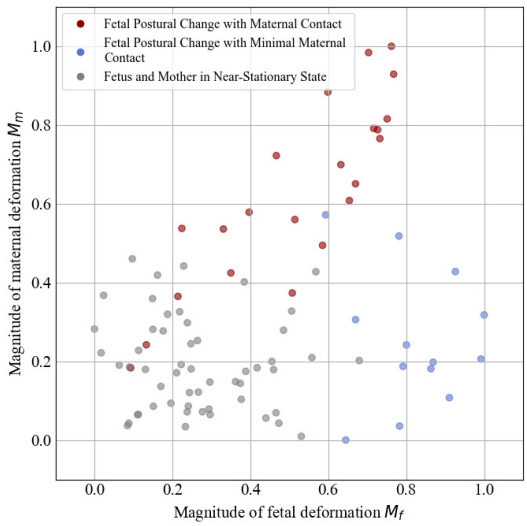

Fig. 6: Fetal and maternal deformation map. M_m represents the maternal deformation, denoted by $M(s = 166)$, and M_f represents the fetal deformation, which is the integration of $M(s = 33)$, $M(s = 92)$, and $M(s = 182)$ using PCA.

C. Construction of Fetal-Maternal Deformation Map

The time-series changes of the constructed fetal and maternal axis deformation magnitudes are shown in Fig. 5. This graph also overlays the timing of fetal movements. These results are normalized and then processed using a 0.1Hz low-pass filter.

Subsequently, the results of plotting each data point on the constructed fetal-maternal deformation map are shown in Fig.6. To represent the deformation patterns and fetal movement characteristics shown by this map, each data point has been manually classified based on the four categories conceptually defined in the Method section, and the results are indicated by the color of each point.

V. DISCUSSION

A. Appropriateness of Shape Description Features and Deformation Extraction

The scale extraction using wavelet variance in this study suggested that it appropriately captures the major shape changes of the fetus and the mother, respectively. The three

scales extracted from the fetal video, $\mathbf{S}_p = \{33, 92, 182\}$, are considered to correspond to subtle movements of fetal limbs ($s = 33$), movements of the trunk ($s = 92$), and large movements such as whole-body extension ($s = 182$). This supports the MRF method's ability to comprehensively capture fetal deformations across diverse anatomical scales. On the other hand, the scale extracted from the maternal video ($s = 166$) is considered to correspond to the shorter dimension of the maternal body. This result can be interpreted as the main response when fetal movement is transmitted to the mother being easily captured at this scale. These extracted sets of scales served as an appropriate analytical basis for the subsequent deformation magnitude calculation.

B. Validity of Deformation Estimation Method

To evaluate whether the constructed fetal and maternal axis deformation magnitudes are effective features for identifying fetal movements, a comparison with time-series data was performed. As shown in Fig. 5, it was confirmed that the local maxima in the time series of each deformation magnitude generally appeared simultaneously with the fetal movements observed in the input video. This result clarified that the deformation magnitudes estimated by this method are indeed synchronized with fetal movements and the accompanying maternal response.

Furthermore, a detailed analysis of the time-series data revealed the following two patterns of fetal movement and their relationship with deformation magnitudes. Each pattern is indicated as (1) and (2) in Fig.5. (1) The case where fetal deformation lags behind maternal deformation corresponds to a flexion posture. This is a case where maternal deformation peaks at the moment the fetus separates from the maternal abdominal wall, and then the maximum of fetal deformation appears later as the fetus continues to deform internally. This is thought to correspond to movements where the fetus gains space by moving away from the abdominal wall and then further stretches its body or changes its posture within that space. In contrast, (2) the case where the maxima of both axes are simultaneous corresponds to an extension posture. This suggests that the fetal movement is directly and strongly transmitted to the maternal abdominal wall. It is presumed that when the fetus gives a physical impact to the mother, like a kick, the deformation of both the fetus and the mother reaches its peak almost simultaneously, and such fetal movements are considered to be deformations that are easily perceived by the mother.

These findings clarify the relationship between the nature of the fetal movement that occurs and the resulting deformation magnitudes of the fetus and the mother.

C. Analysis of Fetal Movement Patterns in the Fetal-Maternal Deformation Map

Fig. 6 shows the constructed fetal-maternal deformation map, visually representing the simultaneous deformation state of the fetus and the mother. Since this simulation video did not contain data corresponding to "Maternal deformation not caused by fetal movement," only the following three categories of data were distributed on this map.

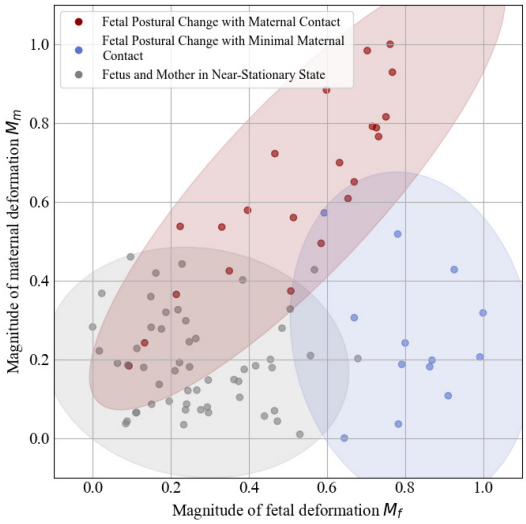

Fig. 7: Fetal and maternal deformation map. M_m represents the maternal deformation, denoted by $M(s = 166)$, and M_f represents the fetal deformation, which is the integration of $M(s = 33)$, $M(s = 92)$, and $M(s = 182)$ using PCA.The red area shows Prominent maternal deformation caused by fetal movement, the blue area shows Fetal movement with minimal maternal contact, and the gray area shows Fetus and Mother in Near-Stationary State.

Data points classified as "Prominent maternal deformation caused by fetal movement" showed a tendency to concentrate in the upper-right region of the map. This region indicates that both fetal deformation (X-axis) and maternal deformation (Y-axis) are large, reflecting a state where fetal activity is strongly transmitted to the maternal abdominal wall. Among the fetal movement patterns, (2) fetal movements where the maxima of both axes are simultaneous were classified into this category.

Data points classified as "Fetal movement with minimal maternal contact" showed a tendency to distribute in the lower-right region of the map. This region suggests that while fetal deformation is large, maternal deformation is small. This is considered to objectively capture situations where the fetus is actively moving, but the movement is not sufficiently transmitted to the abdominal wall, making it difficult for the mother to perceive the fetal movement. Among the fetal movement patterns, (1) fetal movements where fetal deformation lags behind maternal deformation were classified into this category.

Data points classified as "Near-stationary state of both fetus and mother" were concentrated in the lower-left region of the map. This region accurately represents a state where both fetal and maternal deformation are small, indicating no significant fetal movement or maternal movement.

To evaluate the discriminability of each state, Fig. 7 visualizes ellipses enclosing data points for each class, using

the square root of 5.991, which is the value of the 95% confidence interval of the chi-squared distribution (with 2 degrees of freedom). This showed the possibility that each class can be categorized, despite some overlap between them.

In this video, the category "Maternal deformation not caused by fetal movement" was not observed on the map. However, it is expected that by using actual ultrasound data in the future, maternal deformation due to the mother's own movements or external influences will be plotted in the region where only the Y-axis of the map is large (upper-left region). This would enable clear distinction between fetal-derived movements and maternal-derived movements, preventing misidentification of fetal movements.

These results suggest that the map proposed in this study clearly demonstrates the relationship in fetal and maternal deformation, leading to the potential for objective classification of fetal movements based on future maternal perceptual characteristics. This classification method not only complements subjective maternal fetal kick counting but also clarifies movements that should be actively presented, for example, fetal movements classified as "Prominent maternal deformation caused by fetal movement," especially for mothers who have difficulty perceiving fetal movements. Furthermore, for "Fetal movement with minimal maternal contact" movements, where the fetus is active but difficult to perceive, providing information that the fetus is moving is considered to further contribute to health check-ups and attachment formation support.

VI. CONCLUSIONS

This study proposed a fetal-maternal deformation map aiming to objectively assess fetal movements in perinatal care. This map was constructed by applying the previously established MRF method to simultaneously quantify the deformation magnitudes of the fetus and the maternal abdominal wall from simulated fetal movement videos.

Analysis using this map clearly visualized the relationship between fetal and maternal deformation. Furthermore, it was suggested that patterns of fetal movement that are easily perceived by the mother can be categorized from those that are difficult to perceive, depending on the extent of the impact of fetal movement on the maternal abdominal wall. This represents a new approach to objective assessment that considers not only the presence and intensity of fetal movement but also the mother's perceptual characteristics.

The proposed method is expected to contribute to a more detailed assessment of fetal health and the development of personalized support systems for mothers who are anxious about their perception of fetal movements, thereby improving the quality of perinatal medical care. As future work, we plan to algorithmically determine the category boundaries for each individual, for example, by using Bayesian estimation. In addition, we will verify whether the proposed method can recognize fetal movements using real data (ultrasound videos) and by cross-referencing with mothers' subjective perception reports.

REFERENCES

[1] J. F. Frøen, A. E. P. Heazell, J. V. H. Tveit, E. Saastad, R. C. Fretts, and V. Flenady, "Fetal Movement Assessment," *Seminars in Perinatology*, vol. 32, no. 4, pp. 243–246, Aug. 2008. [Online]. Available: https://www.sciencedirect.com/science/article/pii/S0146000508000475

[2] N. AlAmri and V. Smith, "The effect of formal fetal movement counting on maternal psychological outcomes: A systematic review and meta-analysis," *European Journal of Midwifery*, vol. 6, p. 10, 2022.

[3] "Fetal Movement Counting | Article | GLOWM." [Online]. Available: http://www.glowm.com/article/heading/vol-5--surveillance-of-fetal-wellbeing--fetal-movement-counting/id/411783

[4] G. J. Hofmeyr and N. Novikova, "Management of reported decreased fetal movements for improving pregnancy outcomes," *The Cochrane Database of Systematic Reviews*, vol. 2012, no. 4, p. CD009148, Apr. 2012. [Online]. Available: https://www.ncbi.nlm.nih.gov/pmc/articles/PMC4058897/

[5] B. Bradford, R. Cronin, C. McKinlay, J. Thompson, and L. McCowan, "Maternally perceived fetal movement patterns: The influence of body mass index," *Early Human Development*, vol. 140, p. 104922, Jan. 2020.

[6] N. Nandi and R. Agarwal, "Prospective study of maternal perception of decreased fetal movement in third trimester and evaluation of its correlation with perinatal compromise," *International Journal of Reproduction, Contraception, Obstetrics and Gynecology*, vol. 8, no. 2, pp. 687–691, Jan. 2019. [Online]. Available: https://www.ijrcog.org/index.php/ijrcog/article/view/5879

[7] M. S. A, T. A, K. A, W. B. A, G. L, and W. B, "Reduced fetal movement: factors affecting maternal perception," *The journal of maternal-fetal & neonatal medicine : the official journal of the European Association of Perinatal Medicine, the Federation of Asia and Oceania Perinatal Societies, the International Society of Perinatal Obstetricians*, vol. 29, no. 8, 2016, publisher: J Matern Fetal Neonatal Med. [Online]. Available: https://pubmed.ncbi.nlm.nih.gov/26177055/

[8] E. Ross, "Gestating bodies: sensing foetal movement in first-time pregnancy," *Sociology of Health & Illness*, vol. 41, no. 1, pp. 95–111, Jan. 2019.

[9] M. Mesbah, M. S. Khlif, C. East, J. Smeathers, P. Colditz, and B. Boashash, "Accelerometer-based fetal movement detection," pp. 7877–7880, 2011.

[10] Z. R. Hijazi, S. E. Callan, and C. E. East, "Maternal perception of foetal movement compared with movement detected by real-time ultrasound: An exploratory study," *Australian and New Zealand Journal of Obstetrics and Gynaecology*, vol. 50, no. 2, pp. 144–147, 2010, _eprint: https://obgyn.onlinelibrary.wiley.com/doi/pdf/10.1111/j.1479-828X.2009.01122.x. [Online]. Available: https://onlinelibrary.wiley.com/doi/abs/10.1111/j.1479-828X.2009.01122.x

[11] E. Ergen and B. Ulkar, "CHAPTER 18 - Proprioception and Coordination," in *Clinical Sports Medicine*, W. R. Frontera, S. A. Herring, L. J. Micheli, J. K. Silver, and T. P. Young, Eds. Edinburgh: W.B. Saunders, Jan. 2007, pp. 237–255. [Online]. Available: https://www.sciencedirect.com/science/article/pii/B9781416024439500210

[12] D. J. Tuffnell, R. S. V. Cartmill, and R. J. Lilford, "Fetal movements; factors affecting their perception," *European Journal of Obstetrics & Gynecology and Reproductive Biology*, vol. 39, no. 3, pp. 165–167, May 1991. [Online]. Available: https://www.sciencedirect.com/science/article/pii/002822439190052M

[13] H. Matoba, T. Kusaka, K. Shimatani, and T. Tanaka, "Uncertain Shape and Deformation Recognition Using Wavelet-Based Spatiotemporal Features," *Electronics*, vol. 14, no. 11, p. 2131, Jan. 2025, number: 11 Publisher: Multidisciplinary Digital Publishing Institute. [Online]. Available: https://www.mdpi.com/2079-9292/14/11/2131

[14] D. Kim, H. Kanazawa, and Y. Kuniyoshi, "Simulating a human fetus in soft uterus," pp. 135–141, 2022.